Structural Modifications between Lithium-Diborate Glasses and Melts: Implications for Transport Properties and Melt Fragility

Odile Majérus,*,† Laurent Cormier,† Georges Calas,† and Brigitte Beuneu‡

Laboratoire de Minéralogie Cristallographie de Paris, CNRS UMR 7590, Universités Paris 6 et Paris 7, Institut de Physique du Globe, 4 place Jussieu, 75252 Paris Cedex 05, France and Laboratoire Léon Brillouin, C.E. Saclay, 91191 Gif sur Yvette, France

Received: July 10, 2003; In Final Form: September 4, 2003

The effect of temperature on the alkali environment in melts and in glasses has been investigated in Lithium diborate system by neutron diffraction with isotopic substitution of Li. In situ high-temperature measurements have been performed in glassy and liquid states (1273 K), by use of a vanadium furnace. A well-defined environment extends up to 4 Å around Li in the glass as well as in the melt. However, several structural differences are observed between the melt and the glass. The mean Li−O distance is shortened by −0.02 Å in the melt, and the distribution of Li−B correlations is reduced in width and intensity. As the structure of the glass at 300 K retains that of the melt quenched at Tg, the present neutron diffraction data indicate a continuous reorganization process between the supercooled melt and the liquid state. These temperature-induced structural changes are related to the increased modifying role of Li in diborate melt. Together with the boron coordination change, these modifications imply a non-Arrhenian behavior in transport properties such as ionic diffusion and melt fragility.

Introduction

The local environment of cations in glasses remains widely misunderstood, as suggested by the diversity of structural models used to describe them. The knowledge of the cation-hosting sites, and their distribution within the covalent network, can provide a rationale for understanding the compositional dependence of properties such as ionic transport. According to a common paradigm in glass science, cations are distributed in the interstices of the network, and they either modify this network by breaking its connectivity and introducing nonbridging oxygens (NBO's), or they compensate for the charge deficit of some forming units, such as AlO_4^- or BO_4^-. In the modified random network model (MRN), mobile alkali cations are primarily coordinated to NBO's atoms and lie within percolation channels threading randomly through the network.[1] Recently, neutron diffraction experiments with isotopic substitution in silicate glasses have demonstrated the organization of the cation polyhedra within close-packed domains extending up to 10 Å.[2] However, the distribution of bond lengths and bond angles and the possible structural inhomogeneities imply a great variability of cationic sites in the glass structure, with respect to the sites in crystalline phases. This limits our knowledge on relationships between cations and polymeric network.

The structure of alkali borate glasses is dependent on the molar fraction of alkali oxide. Up to about 35 mol %, alkali oxides contribute to form tetrahedral BO_4^- units. The two-dimensional a−B_2O_3 network becomes cross-linked by covalent bonds and progressively suffers a three-dimensional polymerization. Beyond 35 mol %, alkalis begin to depolymerize the network. Alkalis can thus play either a charge compensating or a modifying role in borate glasses. It is not well understood if these two structural roles imply two distinct distributions of cation hosting sites in the structure. For instance, neutron diffraction with isotopic substitution (NDIS) has shown a different structural surrounding of Li in aluminosilicate and silicate glasses,[3,4] in relation to a compensating or a modifying role, respectively. In alkali borate glasses, far-IR spectra show the existence of two distinct components in the vibrating modes of alkali sites.[5] These components have been assigned to the presence of compensating and modifying positions, according to Molecular Dynamics simulations.[6] However, this interpretation may be questioned by ab initio molecular orbital calculations, which assigned the two absorption bands to two different vibrational modes arising from only one distribution of alkali sites.[7] A model of ionic conduction in Lithium borate glasses ascribed the two types of environments to anionic sites occupied either by one or by two Li ions respectively.[8]

At high temperatures above the glass transition temperature (T_g), the melt or the supercooled melt is able to reach its equilibrium state through continuous structural changes. These configurational changes add contributions to thermodynamic properties such as heat capacity or thermal expansion. They are linked to the non-Arrhenian temperature dependence of viscosity within the framework of the configurational entropy theory.[9] The cationic environment in the melt at high temperature may thus be different from that in the melt quenched at T_g. The effect of temperature on the cationic surrounding has not been much investigated, though this surrounding influences the network structure that becomes frozen in and the properties of the resulting glass. Moreover, the local structure around cations in the melts can provide information on the dynamical processes in which cations are involved, because the local cationic environment is related to the energy barriers for diffusive jumps. Recent work on the diffusional mechanisms in the melt, relying

* To whom correspondence should be addressed. E-mail: Odile.Majerus@lmcp.jussieu.fr.
† Laboratoire de Minéralogie Cristallographie de Paris.
‡ Laboratoire Léon Brillouin.

10.1021/jp0359945 CCC: $25.00
Published on Web 11/04/2003

on the long time scale of NMR spectroscopy, has suggested that cations are involved in the mechanism of bond breaking and reforming of the covalent B−O or Si−O bonds, which cause the liquid to flow.[10] However, some degree of decoupling occurs between cationic diffusion and structural viscous relaxation in the supercooled liquid state.[11]

Recent experimental data and numerical modeling on alkali borate glasses have confirmed that increasing temperature induces a progressive decrease of the BO_4^- fraction,[12,13] as predicted by thermodynamic modeling.[14] This structural modification is described by the following reaction:

$$BO_4 \leftrightarrow BO_3 + NBO \quad (1)$$

The right side of the reaction is favored at high temperature, which implies important structural changes of the network between glassy and liquid states. However, the nature and distribution of the alkali sites in the glass and melt structure are still undetermined, although these elements are expected to play a major role in the reaction. Here, we report results of NDIS of Li performed in situ at high temperature on Li-diborate glass and melt. This composition was chosen because it contains the most important fraction of BO_4^- units in the glass and thus gives rise to marked network structural changes above T_g, as demonstrated by a previous neutron diffraction study.[12] By extracting well-defined Li-centered correlation functions for the glass and for the melt, we show that the mean Li−O distance shortens between glassy and liquid states, which can be related to an increasing modifying role of Li in the borate melt. A comprehensive picture of the structural changes between Li−diborate glasses and melts is proposed and put in relationship with transport properties in these melts.

Experimental Section

Materials Preparation. Two glasses of composition $Li_2O-2B_2O_3$ have been synthesized under dry conditions, using isotopically enriched $^{11}B_2O_3$ to avoid the high absorption of ^{10}B nuclei, and reagent grade powders of $^6LiCO_3$ (95,7% ^6Li) for the first glass and $^7LiCO_3$ (99,94% ^7Li) for the second glass. The ^7Li-enriched glass and the ^6Li-enriched glass are noted 7-LB and 6-LB, respectively. The starting powder mixtures were decarbonated at 700 °C during about 12 h, then melted in a covered Pt crucible at 1020 °C for 20 min. The melts were quenched by rapid immersion of the bottom of the crucible in cool water. This procedure was repeated twice to ensure good homogeneity. A previous chemical analysis of Li-diborate glasses prepared under the same conditions indicated only a weak deviation of the composition from the nominal composition (Majérus et al, to be published). Therefore, we used the nominal diborate composition for the data analysis. Densities were measured by an Archimedes method, with toluene as liquid reference, and correspond to a number density of 0.104 ± 0.001 at $Å^{-3}$. This value agrees with that reported by ref 15. The glass transition temperature has been determined by DSC measurements and has a value of 773 K, while the melt temperature is 1190 K.

Neutron Diffraction Experiments and Data Analysis. We carried out the neutron diffraction experiments on the 7C2 diffractometer at the Orphée reactor of the Laboratoire Léon Brillouin (Orsay, France). This instrument uses hot neutrons of wavelength 0.718 Å, giving access to a Q-range of 0.5−16 $Å^{-1}$. Glass samples were powdered just before the measurement in order to avoid hydration and set in a cylindrical vanadium cell at the center of a cylindrical vanadium furnace. Measurements were performed on the glass and melt at room temperature and 1273 K, respectively. Because of the high absorption cross-section of the ^6Li nucleus, we optimized the experimental conditions for the 6-LB glass to get a convenient signal-to-noise ratio. First, we used a can of lower diameter (6 mm for 6-LB instead of 9 mm for 7-LB) to minimize the neutron path length within the sample. Then, at each temperature, we increased the collection time from 7 to 20 h for the 7-LB and 6-LB samples, respectively. Complementary measurements of the scattering from the empty cans in the furnace at 300 K and at 1273 K, from the empty furnace at 300 K, and from the background were performed for use in the data analysis procedure.

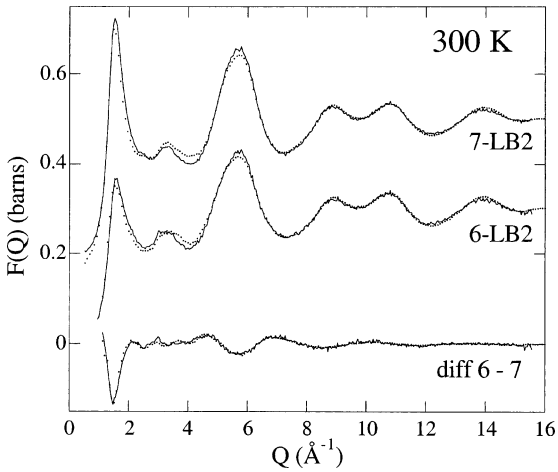

Figure 1. Total structure factors of the 6-LB and 7-LB samples obtained at room temperature on the 7c2 diffractometer (full line) and on the SANDALS diffractometer (bold dashed line) and first difference structure factors calculated from the two sets of data.

The data were corrected from the scattering due to the background, the furnace, and the can and we applied standard corrections from attenuation and multiple scattering.[16] Inelastic scattering in the structure factors was corrected by using the MCGR code, which removes a quadratic background from the data.[17] As the accuracy of the standard analysis was smaller for the 6-LB than that for the 7-LB sample due to the high absorption of the ^6Li nucleus, scattering data of the 6-LB sample were renormalized. For this purpose, we used previous data obtained on SANDALS (ISIS, UK) on 6-LB and 7-LB glasses (Majérus et al, to be published). The structure factor of the 6-LB glass obtained on the 7C2 instrument was rescaled according to the structure factor of the 6-LB glass obtained on SANDALS. Because no reference was available for the data of the 6-LB sample in the liquid state, we renormalized them in the following way. First, we used in the standard analysis an apparent density of 0.0735 at.$Å^{-3}$, instead of the density of 0.090 at.$Å^{-3}$ reported in the literature for the Li-diborate liquid. This parameter change takes into account the fact that the liquid did not fill the entire can, by contrast to the glass powder. Then, renormalization was achieved by using the MCGR code. The quality of the data renormalization was finally checked with the criteria that the total correlation functions $T(r)$ must equal zero at low r, and that the fit of the first peak of the $T(r)$ function, which is assigned to the first B−O pair, must exhibit a Gaussian function with the same parameters as determined in ref 12.[12]

The total structure factors obtained for the glasses on 7C2 are compared to the structure factors from the set of experiments at ISIS (dashed bold lines) in Figure 1. The first difference structure factors $\Delta_{Li}(Q)$ calculated for the two sets of experiments are plotted in the bottom of Figure 1, showing that these

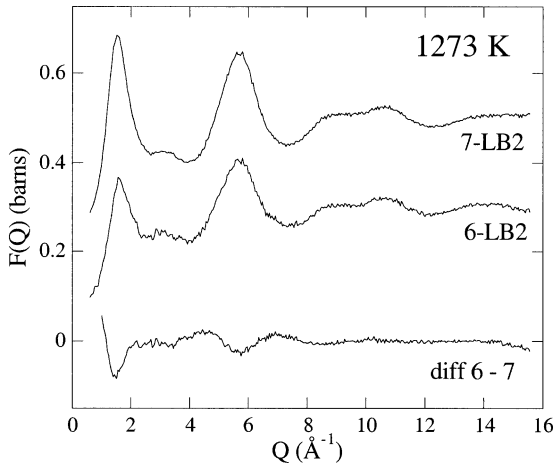

Figure 2. Total structure factors of the 6-LB and 7-LB samples obtained at 1273 K on the 7c2 diffractometer and corresponding first difference structure factor.

two difference signals are identical. Because of the damping of the oscillations in the liquid state, the statistical errors in the measurements at 1273 K are larger than those at lower temperatures, but this does not prevent extraction of a good experimental signal for the liquid (Figure 2).

Diffraction Notation. The total structure factor $F(Q)$ is the distinct scattering term of the total neutron cross section. It can be written in the Faber−Ziman formalism as

$$F_T(Q) = \sum_{\alpha,\beta}^{n,n} c_\alpha c_\beta b_\alpha b_\beta (A_{\alpha\beta}(Q) - 1) \quad (2)$$

where $A_{\alpha\beta}$ are the Faber-Ziman partial structure factors, c_α and c_β are the atomic concentrations of element α and β, respectively, and b_α and b_β are the coherent neutron scattering lengths.

The total radial distribution function $G(r)$ is then obtained by Fourier transformation of $F(Q)$. $G(r)$ can also be written as the neutron weighted sum of all the partial pair distribution functions $g_{\alpha\beta}(r)$.

$$G(r) = \sum_{\alpha,\beta}^{n,n} c_\alpha c_\beta b_\alpha b_\beta (g_{\alpha\beta}(r) - 1) \quad (3)$$

We define the total correlation function $T(r)$ as

$$T(r) = 4\pi\rho_0 r(G(r) + (\sum_i c_i b_i)^2) \quad (4)$$

The difference between the total structure factors of the 6-LB and 7-LB samples allows the cancellation of the identical terms (B−B, B−O and O−O) and gives a weighted sum of the Li-centered Faber-Ziman partial structure factors

$$\Delta_{Li}(Q) = 2 \sum_{\alpha \neq Li} c_\alpha c_{Li} b_\alpha (b_{6_{Li}} - b_{7_{Li}})(A_{\alpha_{Li}}(Q) - 1) + c_{Li}^2 (b_{6_{Li}}^2 - b_{7_{Li}}^2) A_{LiLi}(Q) \quad (5)$$

The Fourier transformation of $\Delta_{Li}(Q)$ gives a Li-centered correlation function $T_{Li}(r)$

$$T_{Li}(r) = 4\pi\rho_0 r G_{Li}(r) + T_{Li}^o(r) \quad (6)$$

TABLE 1: Neutron Weighting Factors for Each Atomic Pair in the Total Structure Factors of Samples 6-LB and 7-LB (eq 2) and in the First Difference Function $\Delta_{Li}(Q)$ (eq 5)

	B−B	B−O	B−Li	O−O	O−Li	Li−Li
6-LB	0.04154	0.12728	0.011405	0.09764	0.017485	0.00072
7-LB	0.04154	0.12728	−0.01391	0.09764	−0.02132	0.00116
ΔLi	0	0	0.01304	0	0.02029	−0.00020

with

$$G_{Li}(r) = 2 \sum_{\alpha \neq Li} c_\alpha c_{Li} b_\alpha (b_{6_{Li}} - b_{7_{Li}})(g_{\alpha_{Li}}(r) - 1) + c_{Li}^2 (b_{6_{Li}}^2 - b_{7_{Li}}^2) g_{LiLi}(r) \quad (7)$$

$$T_{Li}^0(r) = 4\pi\rho_0 r[\sum_{\alpha \neq Li} c_{Li} c_\alpha (b_{6_{Li}} - b_{7_{Li}}) + c_{Li}^2 (b_{6_{Li}}^2 - b_{7_{Li}}^2)] \quad (8)$$

The neutron weighting factors for each atomic pair in the total structure factors and in the first difference are given in Table 1. They allow to evaluate the different pair contributions in the scattering data.

Results

Total Functions. The total structure factors of the 6-LB and 7-LB samples at 300 and 1273 K are presented in Figure 1 and Figure 2, respectively. At large Q values ($Q > 6$ Å^{-1}), the signal is dominated by correlations within planar BO_3 triangles and BO_4 tetrahedra. The features at low-Q values are mainly related to the intermediate-range order, which may involve preferred arrangements between borate units and/or alkali ions. The low-Q range is characterized by a peak at 1.53 Å^{-1} for the 7-LB glass and 1.55 Å^{-1} for the 6-LB glass. A further, weak peak occurs between 3 and 4 Å^{-1} in both glasses. These two features are present in the pure B_2O_3 glass, indicating that addition of Li_2O does not affect much the intermediate-range order of the B_2O_3 glass.[18] However, a contribution in the first peak resulting from the Li correlations is evidenced by a negative peak at 1.50 Å^{-1} in the first difference structure factor, $\Delta_{Li}(Q)$ (see later). With increasing temperature, we mainly observe a damping of the oscillations. The first peak does not vary in position, whereas its width becomes broader, due to the thermal and structural damping of the density oscillations on the medium-range scale.

The total correlation functions are dominated by the contributions due to the B−O network (Figure 3). Structural oscillations are clearly discernible up to about 6 Å. The first peak at ∼1.40 Å and the second peak at ∼2.45 Å are assigned to the B−O and O−O correlations within the BO_3 and BO_4 units, respectively, with a minor contribution from the first B−B correlation in the second peak.[18] The well-defined third peak at 3.65 Å, and the fourth peak at 4.5 Å are assigned to B−O2, where O2 refers to the second O neighbors, and O−O2, respectively. They indicate a network ordering beyond the basic units (i.e., the presence of superstructural units (borate rings) which have been evidenced in borate glasses).[19] With increasing temperature, the first B−O peak is shifted by 0.01 Å toward the low-r side, while the second peak (O−O and B−B) undergoes a shift toward the high-r side and a decrease in intensity. These changes correspond to a decrease of the proportion of boron in BO_4 units from 45% in the glass to about 30% in the melt.[12]

First Difference Functions. The first difference structure factors at 300 and 1273 K are presented in Figure 1 and Figure 2, respectively. The contributions of the Li−O and Li−B pairs account for about two-third and one-third, respectively (the Li−Li weighting factor is almost negligible). A single oscillation

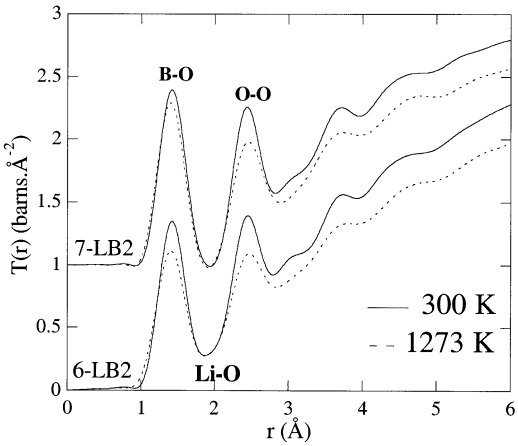

Figure 3. Total correlation functions obtained by Fourier Transform of the total structure factors $F(Q)$ from the 7c2 diffractometer experiments at 300 and 1273 K. The $F(Q)$ were modified by a Lorch function and Fourier transformed with a data interval of 0.6−15.56 Å^{-1}.

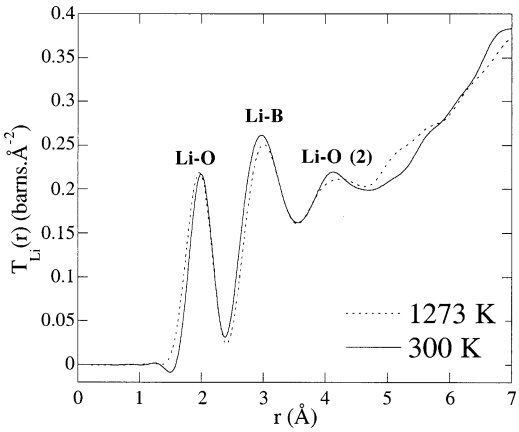

Figure 4. Li-centered correlation functions at 300 and 1273 K, obtained by Fourier Transform (FT) of the first difference structure factor with a data interval of 1.0−14.32 Å^{-1}. Oscillations at low r were removed by an inverse Fourier Transform procedure. A Lorch modification was used in the FT calculation.

dominates the signal at high-Q values (Q > 8 Å^{-1}), which is due to the contribution of the Li−O short distances. At low Q values, a first peak appears at the same position as the first peak in the total structure factors. This suggests a medium-range structural arrangement involving both the B−O network and the Li environment, as discussed below. Between 2 and 4 Å^{-1}, the signal almost cancels, which is likely the result of strong anti-phase interference between Li−O and Li−B contributions. The features of the structure factors are maintained in the liquid, indicating that the Li−O and Li−B correlations are interfering with about the same periods and relative amplitudes in the glass and in the melt. However, an important damping of the structural oscillations can be observed in the first difference structure factor of the melt.

The Li-centered correlation functions in the glass are shown in Figure 4. The first Li−O distance appears at about 2 Å, in close agreement with a previous neutron diffraction study.[18] A second peak appears at 2.95 Å. In lithium diborate crystal, Li has 6 B neighbors and 2 O neighbors at distances between 2.6 and 3.1 Å. By comparison, we can assign mainly this peak to the first Li−B correlation. The two peaks at 2 and 2.95 Å are well separated, which is strong evidence for a well-defined Li polyhedron in the glass. From these two distances, the mean Li−O−B angle may be estimated at ∼118°. A third peak occurs

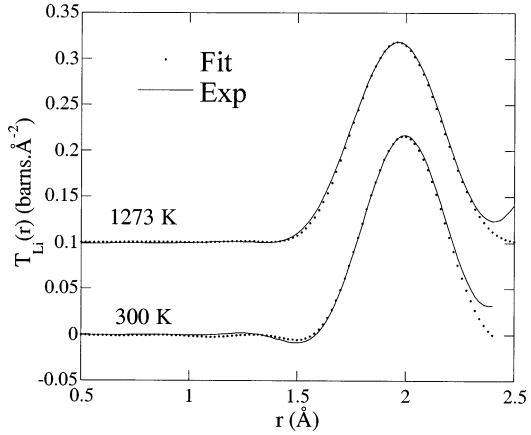

Figure 5. Gaussian fits of the Li−O first peak at 300 and 1273 K.

TABLE 2: Parameters Obtained by Gaussian Fit of the First Peak in the Li-Centered Differential Correlation Functions ($T_{Li}(r)$), Mean Li−B Distances and Mean Li−O−B Bond Angles Calculated from the Mean Li−O, Li−B, and B−O Distances Extracted from Neutron Data (This Study and Study of Ref 12)

T (K)	$N \pm 1.6$	σ ± 0.01 Å	d Li−O ± 0.01 Å	d Li−B ± 0.02 Å	Li−O−B angle (deg)
300	4.9	0.090	1.995	2.95	118
1273	5.4	0.130	1.970	2.99	123

at about 4 Å, and a comparison with the Li-diborate crystal suggests that this feature is mainly due to second Li−O contributions. Beyond this range, Li-centered structural oscillations appear at 7 Å and then at about 12 Å, but their attribution is difficult, due to the overlapping of all Li-centered contributions.

In the melt, a first well-defined Li−O peak appears, which is clearly separated from the other structural features, as in the glass. We find again two other contributions at about 3 and 4 Å, indicating that a medium-range order around the Li ion is maintained. However, significant changes are observed between the liquid and glassy states (Figure 4). With increasing temperature, the position of the first peak (Li−O) is significantly shifted toward the low-r side and the width is broadened. The second peak (Li−B mainly) is shifted by +0.04 Å and becomes narrower and less intense than in the glass. Similarly, the intensity of the third peak decreases. These differences show a modification of the mean Li-cationic site in the liquid with respect to that in the glass.

The first Li−O peak has been fitted by one Gaussian component, convoluted with the Fourier Transform of the Lorch modification function used to calculate the correlation functions. Fits of the first peak for the glass and the melt are shown in Figure 5. The coordination number, N, the Debye−Waller factor, σ, and the mean Li−O distance, d_{Li-O}, are reported in Table 2, along with the mean Li−B distances and Li−O−B bond angles.

At high temperature, the mean Li−O distance decreases by about 0.02 Å. The mean coordination number N is about the same in the glass and in the melt. The value is large, $N = 5 \pm 1.6$, and should be considered with caution. It is affected by errors in the difference method, which result from uncertainties in sample composition and density, and from the analysis of the diffraction data of the absorbing 6-LB sample. The deviation of the $T_{Li}(r)$ function from zero at low r allows an evaluation of this error. This deviation was found to be about 15 and 35% of the T^0_{Li} term (eq 8) in the glass and melt data, respectively. The Debye Waller factor is large in the glass, and increases in

the melt as expected by vibrational and diffusional damping at high temperature.

Discussion

Medium-Range Ordering in Li-Diborate Glass and Melt. The structures at low *Q* values correspond to an ordering at the medium-range scale, whose microscopic origin is not well understood. The variation in intensity of the first *Q*-peak due to the Li isotopic substitution provides some information about the origin of this feature. The first peak of the 6-LB glass, in which Li has a positive scattering length, is less intense than the first peak of the 7-LB glass, in which the scattering length of Li is negative. The Li-centered medium-range ordering appears in the first difference structure factor, with a negative first peak at 1.50 $Å^{-1}$. This dependence on the isotopic composition was also observed in the data of Swenson et al. [18] and supported by a void-based model, according to which the peak results from an ordering of interstitial voids around clusters. As a consequence, its intensity changes if voids are occupied by foreign atoms, for instance, Li cations in the Li-diborate glass. A comparison with the crystalline Li-diborate permits to be more specific about the first peak by suggesting that it arises from "quasi-Bragg planes".[20] By analogy with the (112) crystalline plane structure in the Li-diborate crystal, the Li atoms in the glass lie between the pseudo borate planes, giving anti-phase contributions to the first peak with respect to the B−O contributions. These models point out the structural relationship between cationic ordering and borate network topology, based on an alternation of Li and B−O centered clusters. Moreover, between 2 and 4 $Å^{-1}$, the first difference structure factor $\Delta_{Li}(Q)$ almost cancels. This lack of structural features suggests strong anti-phase interferences between Li−O and Li−B correlations, which are the dominant partial terms in this function. The significance of this lack of structural information in the real space is an alternate ordering of Li and B/O atoms. By use of the relationship $L = 2*\pi/Q$, the correlation length for the fluctuations should be about $L = 4.1$ Å, which equals the distance between (112) planes in crystalline Li-diborate.

In the liquid, the first peak is still discernible in the total structure factors, and similarly, the negative low-*Q* peak still exists in the first difference data. Besides, the signal cancellation between 2 and 4 $Å^{-1}$ is maintained. This brings out that an alternation of Li and B−O centered structural components exists in the melt as in the glass. The first peak becomes broader, which indicates that the length over which the relevant correlations are maintained is less extended. We cannot observe any shift of its position, so that no thermal expansion effect is apparent in the diffraction data for these medium-range arrangements.

The Li Environment in Li-Diborate Glass. The mean Li−O distance in the glass is 1.99 ± 0.01 Å, in agreement with a previous neutron diffraction study.[18] The mean Li−O distance for Li in tetrahedral site, the most frequent Li-coordination in crystals, is 1.98 Å.[21] In crystalline Li-diborate, Li occurs in a distorted 4-fold site, with a mean Li−O distance of 2.05 Å.[22] According to the bond-valence − bond-length relationship,[23] the four oxygens account for a total valence of 0.83. A fifth oxygen exists at 2.63 Å, and a total number of seven oxygen atoms lie within a radius of 3 Å from the Li center, so that the achieved bond-valence for Li is 1. Fivefold and 6-fold coordinated sites in Li-bearing crystals give Li−O distances ranging from 2.05 to 2.30 Å.[21] The mean Li−O distance of 1.99 Å found in the glass can thus be related to an average tetrahedral site. The Gaussian fit of the Li−O peak (Table 2) gives a large value for the coordination number ($N = 4.9$) and for the Debye Waller factor ($\sigma = 0.090$ Å). Both parameters are affected by an important uncertainty, due to systematic errors. However, they suggest a distorted Li average site. Similarly, Li atoms occur in distorted tetrahedral sites in Li-aluminosilicate [3] and Li-disilicate glasses,[4] with one oxygen of the 4-fold-coordination sphere distant by +0.3 Å and +0.2 Å, respectively. Moreover, the Li environment obtained by molecular dynamics (MD) simulations on Li borate glasses indicates that Li cations are located in various distorted sites with 4 to 7−8 oxygen neighbors.[6]

According to the glass composition, the total negative charge in the Li-diborate glass is 0.5 per boron atom, which means that 50% of the boron polyhedra carry one negative charge. NMR and neutron diffraction data have shown that about 45% of boron atoms occurs in BO_4^- units in the Li-diborate glass.[12,24] This implies that 90% of the total negative charge is carried by the BO_4^- units and the other 10% correspond to NBO's on BO_3 units. Therefore, the Li sites that have been described above correspond mainly to charge compensating positions expected in the vicinity of the BO_4^- tetrahedra. Two different Li sites have been described by infrared spectroscopy and MD in Li-borate glasses.[5,6] The compensating positions were identified with the largest coordinated sites (7−8 oxygen neighbors) having a mean Li−O distance of 2.12 Å and no participation of nonbridging oxygens. According to our data, 4-fold-coordinated Li-sites prevail in the diborate glass with Li−O distances that are shorter than the distances proposed for the compensating site. This suggests that the two types of Li sites (related to modifying and compensating positions) are not as distinct as indicated by MD and that Li may occur in a broad site distribution rather than in two types of sites in Li borate glasses. Similarly, only slight differences have been reported for the local order around Li in a modifying or a compensating role in $Li_2Si_2O_5$ and $LiAlSiO_4$ glasses. The main difference lies in the Li−O distances, which equal 2.02 Å (three O atoms at 1.97 Å and one O atom at 2.20 Å) in the $Li_2Si_2O_5$ glass, and 2.10 Å in $LiAlSiO_4$ glass.[3,4]

The Li−B peak at 2.95 Å and the mean Li−O−B angle of 118° can be compared with models of corner- and edge-connections between Li ions and borate units. A geometrical calculation based on mean Li−O and B−O distances of 2.0 and 1.47 Å, respectively, gives a Li−B distance value of 2.45 Å for an edge-connection between the Li site and BO_4^- unit. In the crystalline Li-diborate, Li is edge-connected to one BO_4 unit, with Li−O and Li−B distances of 2.10 and 2.67 Å, respectively, giving two Li−O−B angles of about 95°, while the mean Li−O−B angle is 112.3°. Therefore, the mean Li−B distance and Li−O−B angle in the glass suggest that most Li polyhedra are corner-connected to the boron units. A minor contribution of connections by edge to BO_4- units may occur, but it should be less systematic than that in the crystal. As a consequence, Li and B atoms appear more distant in the glass than in the crystal.

Modification of the Li Environment in the Melt. The most striking feature in the Li-centered correlation function for the melt is the shortening of the Li−O distance from 1.99 to 1.97 Å. The mean linear expansion coefficient of Li−O tetrahedra is about 20×10^{-6} K^{-1} [25] between 300 and 1300 K. Thus, the Li−O distance should have reached the value of 2.04 Å in the melt, if the mean Li-site existing in the glass was maintained. Because such a thermal expansion is not observed in our neutron diffraction data, the Li environment should undergo an important modification upon melting. The low mean Li−O distance

indicates an important proportion of short Li−O bonds in the melt with respect to the glass. These short bonds are most likely Li−NBO bonds (e.g., the Li−BO distance is about 0.14 Å longer than the Li−NBO distance in $Li_2Si_2O_5$ crystal[26]). It thus indicates a high number of NBO's in the coordination sphere of Li in the melt. In situ high-temperature neutron diffraction experiments [12] have estimated a proportion of 30% BO_4^- units in the melt, so that the total negative charge is distributed between BO_4^- units to 60% and NBO's to 40%. Consequently, 40% of the Li ions at least are in a modifying structural position in the melt, compared with only 10% in the glass. The increased number of NBO's found in the coordination sphere of Li in the melt is consistent with this increased modifying role. Besides, the large values of the Debye Waller factor (0.130 Å) and coordination number (5.4) suggest that these short Li−O bonds coexist with larger ones (i.e., Li sites are strongly distorted).

Another important change is the increase of the mean Li−B distance by about +0.04 Å in the melt. Subsequently, the mean Li−O−B angle slightly rises up to 123°. This evolution shows a modification in the connection of the Li polyhedra with the borate network, resulting in a greater separation of the Li ions from the B atoms in the melt. Again, the evolution of Li toward a more modifying role helps rationalizing the observed changes. In their compensating role, Li ions are located in the interstitial voids of the borate network and may establish connections by edge with the negatively charged units. In their modifying role, Li ions disrupt the borate network and are located in sites partly connected via NBO's to the borate units. The Li−(NBO)−B angles are likely to be larger than the Li−(BO)−B angles, because NBO's are linked to only two atoms, while BO's are linked to three atoms, the two boron atoms and the Li cation. Due to simple steric hindrance, the mean Li−O−B angle may thus be larger for these Li modifying ions, resulting in a higher Li−B mean distance. Furthermore, we observe that the Li−B peak presents an apparent narrowing, while a broadening should be expected due to the thermal disordering, and an important decrease in intensity. These findings are consistent with a lower number of Li−B pairs, indicating that Li-polyhedra are less connected to the borate network in the melt than in the glass.

However, it may be emphasized that the structural modifications evidenced in this study do not reflect abrupt structural changes at the glass transition. As shown by previous neutron diffraction studies,[12] the structure of the glass at 300 K retains that of the melt quenched at T_g. The present neutron diffraction data indicate a continuous reorganization process between the supercooled melt and the liquid state.

Relationship Between Local Structure of Li and Ionic Diffusion. Neutron diffraction data indicate that the decreasing proportion of BO_4^- tetrahedra in the melt relative to the glass and the simultaneous increase of NBO's have consequences on the Li local environment. This structural modification should affect the magnitude of ionic diffusion and its temperature dependence. The alkali diffusion in borate glasses is a thermally activated process which can be described by Arrhenius equations, while above T_g, a non-Arrhenius enhancement of the Na diffusivity has been reported, from 1.4×10^{-12} $m^2 \cdot s^{-1}$ in the glass (750 K) to 7×10^{-12} $m^2 \cdot s^{-1}$ in the supercooled liquid state (800 K), through direct measurements of ^{22}Na diffusion.[27] Furthermore, NMR spin−lattice relaxation time measurements[28] have shown that the number of mobile Na ions in Na borate glasses increases with temperature from glassy to liquid state. This non-Arrhenius behavior of the alkali mobility above T_g may be related to the increasing number of alkali in modifying positions in the melt. This is corroborated by the fact that Na diffusion in silicate glasses, where all Na ions are in a modifying position, is faster than in borate glasses by about 1 order of magnitude at similar alkali content and temperature (about 10^{-11} $m^2 \cdot s^{-1}$ compared with 10^{-12} $m^2 \cdot s^{-1}$ in alkali disilicate glasses and diborate glasses, respectively, at T_g).[27] However, the enhanced diffusivity of cations in melts and the non-Arrhenius temperature dependence of this diffusivity are also explained by considering that potential energy barriers vanish with time due to local reorganizations of the neighboring atoms.[29] A less ambiguous interpretation of the structural dependence of the alkali-diffusivity would require to separate this relaxation effect from that of the average alkali environment.

The modifying position is characterized by the participation of NBO's to the Li polyhedra, as confirmed by our neutron diffraction data. A relationship appears between the enhanced mobility of Li ions in the melt and the presence of NBO's in their local environment. Such a relationship has been evidenced by Molecular Dynamics simulation in alkali borate,[6] silicate,[30,31] and phosphate glasses.[32] In the Modified Random Network model, the influence of the NBO neighbors on the alkali diffusion has been accounted for by the existence of percolating regions enriched in alkalis and NBO's. These regions provide diffusive pathways for the alkali ions, moving through energetically favored "intra-channel" hopping.[33,34] MD models obtained for Li borate glasses and melts[6] have put in evidence such a spatial segregation of Li and NBO's. The Li-diborate glass contains few NBO's, and neutron diffraction data are not able to detect whether these NBO's are segregated around Li ions. The situation is different in the melt, which contains more NBO's than in the glass. The magnitude of the changes in the Li-centered correlation function for the melt appears to be large, in particular for the Li−O mean distance. Indeed, according to the decrease of the proportion of BO_4^- tetrahedra with temperature,[12] 30% of Li ions may change from a compensating to a modifying position between glassy and liquid states. This will give a shift of the Li−O mean distance by −0.03 Å, using the average Li−O distances determined for a compensating or a modifying position.[3,4] The Li−O thermal expansion (20×10^{-6} K^{-1}) will cancel this negative shift in the melt. The observation of a short Li−O distance suggests a high number of NBO's associated with the Li atoms and thus a segregation of Li and NBO's in the melt. A direct determination of Li segregation is not possible on neutron diffraction data, because the weight of the Li−Li partial is too weak to be discernible in the difference correlation function. However, a segregation of Li ions in the melt may be further supported by the evolution of the second peak in the difference correlation function, which indicates less connections between Li and the borate network in the melt.

Relation to Melt Fragility. Compared to alkali silicate and pure B_2O_3 melts, alkali borate melts are fragile systems, because their viscosity strongly deviates from the Arrhenius temperature dependence near T_g.[35] At $T = 1.1 \cdot T_g$, the viscosity drops by 5 and 3 orders of magnitude in $25Li_2O$-$75B_2O_3$ and Na_2O-$2SiO_2$ compositions, respectively.[36] Only anorthite ($CaAl_2Si_2O_8$) and diopside ($CaMgSi_2O_6$) melts have comparable fragilities to that of alkali borate melts. According to the Adam and Gibbs theory, the structural relaxation in melts becomes more cooperative as the temperature decreases up to the glass transition, which results in a decreasing configurational entropy.[37] Fragile melts have their configurational entropy, which rapidly drops at the glass transition contrary to strong melts,[38] indicating that the cooperativity in structural relaxation sharply increases. In alkali borate melts, the structural relaxation during the viscous flow occurs through borate species conversion assisted by alkali

migration.[39] The source of configurational entropy lies in the boron coordination change and accompanying changes in alkali environment, which occur above the glass transition. Indeed, the heat capacity difference associated to this structural rearrangement accounts for the most part of the total heat capacity difference at T_g.[12,13] This species exchange can be written as

$$BO_4 + Li^{comp} \leftrightarrow BO_3 + NBO + Li^{mod} \quad (9)$$

where the Li^{comp} and Li^{mod} notations refer to the compensating and modifying positions for Li, respectively, and are used to take into account the changes in Li environment associated with the BO_4/BO_3 exchange process. Our data clarify these changes in the Li surrounding and provide a structural basis for the cooperativity increase predicted for this process near T_g. In particular, the evolution of the Li−B peak, which both increases in intensity and becomes broader as temperature decreases from 1273 to 300 K, suggests that Li ions are more closely linked to the borate network in the glass than in the melt. Besides, alkali silicate melts are less fragile than alkali borate melts, because they do not give rise to such important structural changes with temperature. Accordingly, the degree of cooperation between the chemical species during structural relaxation does not vary much with temperature in silicates. The increasing coupling between Li ions and the borate network suggests that the latter constrains, to some extent, the local structure of the former as temperature decreases near the glass transition. In the melt, Li ions appear to be stabilized at the vicinity of NBO's. This preferential relation between Li and NBO's decreases at lower temperature, as boron partially converts to tetrahedral coordination. The driving force for this conversion is not clear and may involve chemical stabilization requirements of both borate species and Li atoms.[40]

Conclusion

In situ neutron diffraction of Li-diborate glass and melt (1273 K) with Li isotopic substitution demonstrates clearly defined structural modifications between borate glasses and melts. The Li−O mean distance is 1.99 ± 0.01 Å in the glass and shortens to 1.97 ± 0.01 Å in the melt, in relation with an enhanced modifying role of Li. The relationship between Li ions and the borate network is also different in glass and melt. This may be understood by a more important contribution of NBO's to the Li coordination shell in the melt than in the glass, which induces higher Li−B distances in the former. As the structure of the glass at 300 K retains that of the melt quenched at Tg, the present neutron diffraction data indicate a continuous reorganization process between the supercooled melt and the liquid state. The strong temperature-induced modification of the relationship between Li and the polymeric network may contribute to the non-Arrhenian increase of the cationic diffusion in alkali borate melts and their unusual fragile character. Numerical modeling is in progress to better constrain the available structural information. This will give new insights into the significance of the structural modifications occurring around cations during melt-to-glass transformations in oxide systems.[41]

Acknowledgment. We are grateful to J.P. Ambroise, L. Galoisy and D.R. Neuville for their help during the data acquisition on the 7C2 spectrometer. The authors thank two anonymous reviewers for helpful comments. This is an IPGP contribution No. 1934.

References and Notes

(1) Greaves, G. N. *Philos. Mag. B* **1989**, *60*, 793−800.
(2) Cormier, L.; Calas, G.; Gaskell, P. H. *Chem. Geol.* **2001**, 349−363.
(3) Cormier, L.; Gaskell, P. H.; Calas, G.; Zhao, J.; Soper, A. K. *Phys. Rev. B* **1998**, *57*, R8067−R8070.
(4) Zhao, J.; Gaskell, P. H.; Cluckie, M. M.; Soper, A. K. *J. Non-Cryst. Solids* **1998**, *232−234*, 721−727.
(5) Kamitsos, E. I.; Patsis, A. P.; Chryssikos, G. D. *J. Non-Cryst. Solids* **1993**, *152*, 246−257.
(6) Varsamis, C.-P. E.; Vegiri, A.; Kamitsos, E. I. *Phys. Rev. B* **2002**, *65*, 104203.
(7) Uchino, T.; Yoko, T. *Solid State Ionics* **1998**, *105*, 91−96.
(8) Elliott, R. J.; Perondi, L.; Barrio, R. A. *J. Non-Cryst. Solids* **1994**, *168*, 167−178.
(9) Richet, P.; Neuville, D. R. Thermodynamics of silicate melts: Configurational properties. In *Thermodynamic Data. Systematics and estimation*; Saxena, S., Ed.; Springer-Verlag: Paris, 1992; pp 132−160.
(10) *Structure, Dynamics and properties of Silicate Melts*; Stebbins, J. F.; McMillan, P. F.; Dingwell, D. B., Eds.; Mineralogical Society of America: Washington, D. C., 1995; Vol. 32, p 615.
(11) Angell, C. A.; Ngai, K. L.; McKenna, G. B.; McMillan, P. F.; Martin, S. W. *J. Appl. Phys.* **2000**, *88*, 3113−3157.
(12) Majérus, O.; Cormier, L.; Calas, G.; Beuneu, B. *Phys. Rev. B* **2003**, *67*, 024210.
(13) Sen, S.; Xu, Z.; Stebbins, J. F. *J. Non-Cryst. Solids* **1998**, *226*, 29−40.
(14) Araujo, R. J. *J. Non-Cryst. Solids* **1983**, *58*, 201−208.
(15) Mazurin, O. V.; Streltsina, M. V.; Shvaiko-Shvaikovskaya, T. P. *Handbook of Glass Data*; Amsterdam, 1985.
(16) Soper, A. K.; Howells, W. S.; Hannon, A. C. *ATLAS − Analysis Time-Of-Flight diffraction data from liquid and amorphous samples*; Rutherford Appleton Laboratory Report, 1989.
(17) Zetterström, P.; McGreevy, R. L. *Physica B* **2000**, *276−278*, 187−188.
(18) Swenson, J.; Borjesson, L.; Howells, W. S. *Phys. Rev. B* **1995**, *52*, 9310.
(19) Krogh-Moe, J. *Phys. Chem. Glasses* **1965**, 46.
(20) Gaskell, P. H. *Low-Q features in diffraction data for borate glasses and crystals- an examination of similarities in medium-range structures; Borate Glasses, crystals and melts*; The Cosener's House, Abingdon, UK, 1997.
(21) Wenger, M.; Armbruster, T. *Eur. J. Mineral.* **1991**, *3*, 387−399.
(22) Krogh-Moe, J. *Acta Crystallogr.* **1968**, 179.
(23) Brese, N. E.; O'Keefe, M. *Acta Crystallogr.* **1991**, *B47*, 192−197.
(24) Zhong, J.; Bray, P. J. *J. Non-Cryst. Solids* **1989**, *111*, 67−76.
(25) Hazen, R. M.; Finger, L. W. *Comparative Crystal Chemistry. Temperature, pressure, composition, and the variation of crystal structure*; Wiley-Interscience: New York, 1982.
(26) Liebau, F. *Zum. Naturf.* **1960**, *B15*, 467.
(27) Schoo, U.; Mehrer, H. *Solid State Ionics* **2000**, *130*, 243−258.
(28) Sen, S.; Stebbins, J. F. *Phys. Rev. B* **1997**, *55*, 3512−3519.
(29) Caillot, E.; Duclot, M. J.; Souquet, J. L.; Levy, M.; Baucke, F. G. K.; Werner, R. D. *Phys. Chem. Glasses* **1994**, *35*, 22−27.
(30) Oviedo, J.; Sanz, J.-F. *Phys. Rev. B* **1998**, *58*, 9047−9053.
(31) Smith, W.; Greaves, G. N.; Gillan, M. J. *J. Non-Cryst. Solids* **1995**, *192−193*, 267−271.
(32) Karthikeyan, A.; Vinatier, P.; Levasseur, A.; Rao, K. J. *J. Phys. Chem. B* **1999**, *103*, 6185.
(33) Greaves, G. N.; Ngai, K. L. *Phys. Rev. B* **1995**, *52*, 6358.
(34) Jund, P.; Kob, W.; Jullien, R. *Phys. Rev. B* **2001**, *64*, 134303.
(35) Chryssikos, G. D.; Duffy, J. A.; Hutchinson, J. M.; Ingram, M. D.; Kamitsos, E. I.; Pappin, A. J. *J. Non-Cryst. Solids* **1994**, *172−174*, 378−383.
(36) Richet, P. *Geochim. Cosmochim. Acta* **1984**, *48*, 471−483.
(37) Adam, G.; Gibbs, J. H. *J. Chem. Phys.* **1965**, *43*, 139.
(38) Angell, C. A. *J. Non-Cryst. Solids* **1991**, 13−31.
(39) Stebbins, J. F.; Ellsworth, S. E. *J. Am. Ceram. Soc.* **1996**, *79*, 2247−56.
(40) Vedishcheva, N. M.; Shakhmatkin, B. A.; Shultz, M. M.; Wright, A. C. Simulation of the Structure of Borate Glasses and Melts on the basis of Thermodynamics. In *Borate glasses, crystals, and melts*; Wright, A. C., Feller, S. A., Hannon, A. C., Eds.; Society of Glass Technology: Sheffield, UK, 1997; p 215.
(41) Calas, G, Brown, G. E., Farges, F., Galoisy, L., Itie, J. P., Polian, A. *Nucl. Instrum. Methods. Phys. Res., Sect. B* **1995**, *97*, 155.